In Situ Assembly of Melittin-PHA Microspheres for Enhancing Therapeutic Efficacy in Cancer Treatment

Xueyu Fan
Hebei University
Chao Zhang
Hebei University
Shuangqing Fu
Hebei University
Shuo Wang
Hebei University
Shuo Ma
Hebei University
Jie Du
Hebei University
Wei Li
Hebei University
Honglei Zhang (zhanghonglei@hbu.edu.cn)
Hebei University

Research Article

Keywords: Melittin, Polyhydroxyalkanoate microsphere, in situ assemble, Stability, Cytotoxicity

Posted Date: January 19th, 2024

DOI: https://doi.org/10.21203/rs.3.rs-3861650/v1

Additional Declarations: No competing interests reported.

Abstract

Amphiphilic cationic peptide (ACP) is a widely studied biofilm-active peptide that has great potential in cancer treatment. However, poor stability, a short half-life, and complex preparation pose significant challenges for practical therapeutic applications. In the current investigation, the amphiphilic peptide Melittin (Mel), recognized for its powerful anticancer properties, was chosen from natural and synthetic ACP, and integrated into a nanostructure by utilizing polyhydroxyalkanoate (PHA) microspheres as carriers to produce Mel-loaded PHA microspheres (Mel@PHA-PhaC). Mel@PHA-PhaC nanostructure was self-assembled in *Escherichia coli*, simplifying its preparation and making it more convenient and high-yield. Mel@PHA-PhaC were spherical, with a particle size of approximately 300 nm, as observed by scanning electron microscopy (SEM) and transmission electron microscopy (TEM). The concentration of Mel in Mel@PHA-PhaC was 4 μg/mg. Mel@PHA-PhaC still maintained good stability after being treated with pancreatic enzymes. Furthermore, *in vitro* experiments demonstrated that Mel@PHA-PhaC enhanced the inhibitory effect on cancer cells compared to free Mel. This study provides insights and guidelines for the development and utilization of peptide delivery systems using PHA microspheres to create stable and improved peptides for cancer therapy.

1. Introduction

Amphiphilic cationic polypeptide (ACP) is a short peptide composed of 12 to 50 amino acid residues, with a molecular weight ranging from 2 to 9 kDa [1]. It has a structure with a hydrophilic head designed to carry a positive charge through lysine and arginine, and a hydrophobic tail containing various levels of hydrophobic amino acids, which make up more than 30% of the total [2]. ACP can be naturally occurring, such as human cathelicidin LL-37 [3], Melittin (Mel) [4], and CM4 [5]. In addition, synthetic cationic peptides (CSA-13 [6], RALA [7], and CMt [8]) have also been rapidly developed [9]. These peptides have demonstrated varying degrees of anticancer activity by killing cells through permeation of the cell membranes and inducing a membranolytic mechanism [10]. However, as research progresses, the use of ACP has encountered some challenges, including poor stability, short half-life, complex preparation, and high cost, which have limited their application in cancer treatment [11]. Therefore, simplifying the preparation of ACP and enhancing its stability is crucial for its application in cancer treatment.

ACP, in its monomer form, has been modified into various specific nanostructures to address the aforementioned issues. Currently, it has been reported that inorganic, organic, and polymer materials are used to transform monomeric ACP into organized nanostructures [12]. Similarly, self-assembled ACP molecules are also formed through careful design [13]. Katarzyna et al. developed a novel magnetic nano-system, MNP@LL-37, comprising an iron oxide core, an aminosilane layer, and the cationic peptide LL-37. This resulted in a more significant decrease in cell viability and a higher rate of apoptosis compared to the free LL-37 peptide [14]. Neelesh R. Soman et al. designed a structure in which Mel, a 26-amino acid peptide, was incorporated into the outer lipid monolayer of a perfluorocarbon (PFC) nanoparticle. PFC nanoparticles, as a unique nanocarrier, not only maintain the structural integrity of Mel, but also extend its duration of Mel by slowly releasing it [15]. Jiang et al. reported the fabrication of cecropins (CECs)-encapsulated zeolitic imidazolate framework 8 (ZIF-8) nanoparticles (CEC@ZIF-8 NPs). The formulation of NPs protected CECs from proteasome degradation, enhanced peptide bioavailability, promoted uptake by HeLa tumor cells, and increased antitumour efficacy compared with free CECs [16]. In addition, through intermolecular interactions, monomeric ACP can self-assemble into nanostructures such as spherical micelles, vesicles, nanotubes, and nanofibers. These structures exhibit better biological activity and higher environmental tolerance than monomers [12]. While numerous studies have contributed to enhancing the biological activity and stability of ACP, the assembly process is quite complex and still necessitates peptide purification prior to

nanostructure assembly. This increases preparation costs and is a significant barrier to mass production. If there is a preparation process for nanopeptides that integrates the purification and assembly process of ACP, it will greatly simplify production and enhance the application prospects of ACP.

Polyhydroxyalkanoate (PHA) microspheres are specific nanostructures formed through the self-assembly of polymers and proteins produced in microorganisms. They possess the characteristics of easy functionalization, high stability, and good dispersion [17]. Hydrophobic polyester chains are situated within the microspheres, while PHA membrane-binding proteins such as PHA polymerase (PhaC) and PHA granule-binding protein (PhaP) are embedded or attached to the outer layer [18]. These membrane-binding proteins are linked to exogenous target proteins through fusion, enabling the direct production of PHA microspheres with surface-bound target proteins in the recombinant strains [19]. Since microspheres are present as independent inclusions in microbial cells, they can be easily separated from cells by disruption and centrifugation. These methods are considered to be effective strategies for the efficient and large-scale preparation of microspheres [20].

In this study, cationic peptide-loaded PHA microspheres were designed and produced using recombinant *Escherichia coli*, and their anticancer activity was evaluated. To accomplish this, an outstanding ACP named Mel was chosen from a pool of candidates from Mel, CM4, CM, and RALA using MTT. The Mel gene was inserted into a plasmid expression system to produce PHA microspheres, and the plasmid was then transformed into *E. coli*. The Mel-loaded PHA microspheres obtained through sonication and centrifugation of *E. coli* were characterized using scanning electron microscopy (SEM) and transmission electron microscopy (TEM). SDS-PAGE and greyscale analysis were used to quantitatively evaluate the Mel on the surface of the microspheres. Furthermore, the stability of these microspheres to pancreatic enzymes and high temperatures was studied. The anticancer activity of the microspheres was also evaluated on different types of cancer cells, and the mechanism of apoptosis was explored. The one-step synthesis of ACP, which self-assembles into nanostructures in microorganisms, greatly simplifies the preparation of peptide nanocomplexes, improves the overall utilization efficiency of peptides, and facilitates the large-scale production of peptide nanocomplexes.

2. Materials and methods

2.1. Materials

Tryptone, yeast extract, sodium chloride, agarose, chloramphenicol, kanamycin, isopropyl-β-D-galactoside thioglycoside (IPTG), glucose, sodium lauryl sulfate (SDS), 30% acrylamide, bovine serum albumin (BSA), imidazole, Sudan black, safranin O, phosphate buffer (PBS), 100 × penicillin/streptomycin solution, and thiazole blue (MTT) were purchased from Sangon Biotech Co., Ltd. (Shanghai, China). Ammonium persulfate (AP), tetramethylethylenediamine (TEMED), dimethyl sulfoxide (DMSO), absolute ethanol, and glacial acetic acid were purchased from the DAMAO Chemical Reagent Factory (Tianjin, China). Dulbecco's Modified Eagle Medium (DMEM), fetal bovine serum (FBS), and trypsin were purchased from TransGen Biotech (Beijing, China). The EasyPure Plasmid MiniPrep Kit, Plasmid Cartridge Gel Recovery Kit, and PCR Product Recovery Kit were purchased from Sangon Biotech Co., Ltd. (Shanghai, China). Mel, CM4, CMt, and RALA peptides were also synthesized by Sangon Biotech Co., Ltd. (Shanghai, China).

2.2 Bacterial strains, growth conditions, and cell culture

The *E. coli* (DH5α) used in this study underwent standard cloning procedures and was grown in Luria-Bertani (LB) medium at 37 ℃. *E. coli* BL21 (DE3) was utilized for the production of the microspheres. When necessary,

antibiotics were added to the LB medium at the following concentrations: chloramphenicol (100 μg/mL) and kanamycin (100 μg/mL).

The human breast cancer cell line MCF-7, human hepatoma cell line HepG2, human pancreatic cancer cell line Aspc-1, human cervical cancer cell line HeLa, and human gastric cancer cell line MGC-803 cells were obtained from the Chinese Academy of Sciences cell bank (Shanghai, China). The cells were incubated in a cell culture medium containing DMEM (89%), FBS (10%), and 0.1 mg/mL penicillin-streptomycin. Cells were cultured at 37 ℃ in a humidified incubator with 5% CO_2.

2.3 Screening of cationic peptide with high anticancer activity

The effect of various free peptides (Mel, CM4, CMt, RALA) on the viability of cancer cell lines (HepG2, MCF-7, Hela, MGC-803, Aspc-1) was assessed using the MTT assay to identify peptides with the most potent anticancer activity [21]. Briefly, 7 × 10^3 cells/well were seeded into 96-well plates in a 5% CO_2; and incubated at 37 ℃ for 12 h to allow the cells to adhere (the wells at the edges were filled with sterile PBS). Furthermore, the spent media was aspirated from the attached cells and washed twice with 1 × sterile PBS. Different concentrations of peptide (1, 3, and 5 μmol/L) solutions were prepared in DMEM medium and added to the respective wells. Control wells without peptides were also set up. After 24 h of incubation, 500 μg/mL of MTT was added to each well and incubated for 4 h. Subsequently, the MTT dye was carefully removed, and the formazan crystals were dissolved in DMSO. Absorbance was measured at 490 nm using a Synergy HTX multifunctional microplate detector (Biotek, Vermont, USA). Control cells without peptide treatment were kept separate to calculate the percentage of cell viability. The dose–response graph was plotted by calculating the percent cell viability using the following formula:

$$\text{Cell viability} = \frac{\text{OD490(sample)} - \text{OD490(blank)}}{\text{OD490(control)} - \text{OD490(blank)}} \times 100\%$$

Additionally, an online calculator (https://www.aatbio.com/tools/ic50-calculator) was utilized to calculate the IC50 values for the four free peptides.

2.4 Construction of Mel@PHA-PhaC microspheres with a SUMO tag assembled in E. coli

A plasmid of pACYCD uet-1 *phaAB* & *sumo-mel-phaC* was constructed. The primers used in the experiment are listed in Table 1. The *phaA*, *phaB*, and *phaC* genes from *Ralstonia eutropha* were inserted into the pET-28a plasmid at appropriate sites to create the pET-28a *phaCAB* plasmid. Using the pET-28a *phaCAB* plasmid as a template, we amplified the *phaA-phaB* nucleic acid sequences by PCR using the *Bam*HI-phaA F and *Hin*dIII-phaB R primers. Additionally, we used the G4S-phaC F and phaC R primers to amplify the *phaC* genes. The *sumo-melittin* (*sumo-mel*) nucleic acid sequence was amplified from the purchased pET-28a *sumo-melittin* plasmid (Sangon Biotech Co., Ltd, Shanghai, China) using the primers sumo-mel F and G4S-sumo-mel R. Subsequently, the *melittin* (*mel*) and *phaC* gene fragments were ligated via a G4S linker. The *phaA-phaB* gene and the pACYCDuet-1 vector plasmid were amplified and then treated with the restriction endonucleases *Bam*HI and *Hin*dIII. The fragments were then ligated to obtain the pACYCDuet-1 *phaAB* plasmid. After digesting the plasmid with the restriction endonucleases *Xho*I and *Kpn*I, the *phaC* and *sumo-mel* gene fragments were seamlessly cloned and linked to create the pACYCDuet-1 *phaAB* & *sumo-mel-phaC* plasmid. The presence of the *sumo-mel-G4S-phaC* insert was confirmed by Sangon Biotech Co., Ltd (Shanghai, China).

Table 1
Primers were utilized in this study.

Target gene	Primer name	Primer sequences(5'→3')
phaA + phaB	BamH - phaA F	CGCGGATCCCATGACTGACGTTGTCATC
	Hind - phaB R	CCCAAGCTTTTAGCCCATATGCAGGC
sumo + melittin	sumo + melittin F	CCACGCGATCGCTGACGTCGGTACCATGTCGGACTCAGAAGTCAATCAAGAAG
	G4S-sumo + melittin R	CCACCCGACCCACCACCGCCCGAGCCACCGCCACCCTGTTGCCTCTTACGTTTAATCCAAC
phaC	G4S-phaC F	GCTCGGGCGGTGGTGGGTCGGGTGGCGGCGGCTCGATGGCGACCGGCAAAGGCGCGGCAG
	phaC R	CAGCGGTTTCTTTACCAGACTCGAGTTATGCCTTGGCTTTGACGTATCG

The pACYCDuet-1 *phaAB* & *sumo-mel-phaC* plasmids were transformed into *E. coli* BL21 (DE3) competent cells. Single colonies were selected and inoculated into 5 mL of LB medium supplemented with chloramphenicol (100 μg/mL) and incubated at 37 ℃ for 12 h. The overnight culture was then diluted into fresh LB medium at a 1:100 ratio and incubated at 37 ℃ for 3 h until the OD_{600} reached 0.6–0.8. IPTG and glucose were added to achieve final concentrations of 1 mmol/L and 2%, and the synthesis of Mel@PHA-PhaC microspheres with SUMO tags was induced at 20 ℃ for 36 h. The cultures were collected and analyzed using 12% sodium dodecyl sulfate-polyacrylamide gel electrophoresis (SDS-PAGE) to confirm the protein expression. To assess the successful synthesis of Mel@PHA-PhaC microspheres with SUMO tags, the cultures were coated in the center of a clean slide, dried, and fixed. Then, they were stained with Sudan black for 10 min at room temperature and rinsed with 75% ethanol until the solution became colorless. Then, the safranin O solution was added to the glass slide for 1 min, washed, dried, and observed under a microscope. The induced cultures were then prepared as described in the literature. The sections were sliced using an ultramicrotome, transferred to a copper mesh, and analyzed by transmission electron microscopy (TEM) using a Tecnai G2 F20 S-TWIN TEM (FEI, Hillsboro, USA).

2.5 Purification and characterization of Mel@PHA-PhaC microspheres

The Mel@PHA-PhaC microspheres with SUMO tags were isolated using sucrose density gradient centrifugation, following the method described by Wieczorek et al. [23]. Briefly, after 36 h of cultivation in LB medium, the cells were collected and resuspended (m:V = 1: 25) in TBSW buffer (per liter, 60 g NaCl, 8 g KCl, 2 g $MgSO_4 \cdot 7H_2O$, 40 mmol Tris-HCl, pH 7.0). The cell suspension was processed using a high-pressure cell crusher (GEFRAN, Italy) at 900 bar for 15 min, and 12 mL of cell lysate was carefully layered on top of a discontinuous sucrose density gradient solution, which was created by combining 8 mL each of 1.6, 1.3, and 1.0 mol/L sucrose in TBSW. When the cell lysate was centrifuged at 160,000 × g and 4 ℃ for 4 h using an OptimaTM XE-100 ultracentrifuge (Beckman Coulter, California, USA), a Mel@PHA-PhaC microsphere with a SUMO tag layer was obtained between the 1.0 and 1.3 mol/L fractions. The microsphere layer was carefully transferred into the Eppendorf centrifuge tube using a

syringe, and the separated microspheres were suspended in PBS and washed twice with PBS through centrifugation. The extracted microspheres were analyzed using SDS-PAGE to detect the synthesis of the fusion protein (SUMO-Mel-PhaC) and to verify the purity of the fusion protein on its surface. The SUMO tag in the fusion protein was cleaved using the SUMO protease Ulp1, which was purified through Ni^{2+}-NTA chromatography following the procedures outlined in the literature [24]. The microspheres were then digested by purified Ulp1 in a suitable buffer for SUMO protease at 30 ℃ for 1 h to obtain Mel@PHA-PhaC microspheres. The standard SDS-PAGE method (12% gel) was employed to analyze Mel-PhaC. Bovine serum albumin (BSA), which has a molecular weight similar to the Mel-PhaC fusion protein, was used as the standard protein. It was diluted with distilled water to concentrations of 40, 80, 120, 160, and 200 μg/mL. The gel images were scanned using the Tanon 2500 gel imaging system (Tanon, Shanghai, China) and analyzed with ImageJ software, version 1.38 (Bio-Rad, USA). The standard curve was constructed by plotting the concentration of BSA on the x-axis and its corresponding gray value on the y-axis. The concentration of Mel-PhaC protein was then determined using the standard curve.

Characterization of Mel@PHA-PhaC microspheres was conducted using scanning electron microscopy (SEM) with a JEM-ARM200F SEM (JEOL, Tokyo, Japan) and TEM. Microspheres were washed with distilled water to remove buffer salts. The cleaned microspheres were then evenly distributed onto the surface of the silicon wafer and dried in a constant-temperature drying oven at 45 ℃. The morphology and shape were observed using SEM. The microspheres were added to a copper grid covered with a porous carbon film to allow the water to completely evaporate at room temperature. The surface of the air-dried microspheres was stained with a 1% phosphotungstic acid aqueous solution (w/w) for 1 min. Then, they were washed with distilled water and dried at room temperature. TEM was then used to characterize the fusion proteins on the surface of the sphere.

2.6 In vitro cytotoxicity assessment of Mel@PHA-PhaC

The effects of various concentrations of free Mel peptides (1, 2, 3, 4, 5 μmol/L) and Mel@PHA-PhaC microspheres (0.1, 0.5, 1.0, 1.5, 2.0 μmol/L) on the activity of cancer cell lines (MCF-7, HepG2, Aspc-1, Hela, MGC-803) were assessed using the MTT assay. The MTT experimental procedure is the same as in 2.3.

Live/dead staining (BBproExtra®, Nanjing, China) was performed to analyze the effect of various peptide concentrations on cell viability. MCF-7 cells were chosen as representatives for live and dead staining experiments. Briefly, 7×10^3 MCF-7 cells were seeded into 96-well plates and incubated for 24 h. The attached cells were then washed with PBS, and separately supplemented with microspheres and free peptides at a concentration of 1 μmol/L, followed by another 24-hour incubation. Subsequently, the cells were stained according to the manufacturer's instructions and observed using a 1X53 inverted fluorescence microscope (Olympus, Tokyo, Japan).

2.7 Trypsin stability assay

To assess the functional stability of the Mel@PHA-PhaC microspheres, both the microspheres and free peptide were incubated in trypsin at a concentration of 1.0 mg/mL at 37 ℃ for 4 h. The reaction was then halted by heating to 60 ℃ for 20 min. As Aspc-1 cells were the most affected by microspheres, they were chosen for peptide stability experiments. Mel and Mel@PHA-PhaC had a similar effect on Aspc-1 cell viability at a concentration of 2 μmol/L. Hence, peptides at this concentration were used for the MTT assay. The MTT experimental procedure is the same as 2.3.

2.8 Apoptosis

MCF-7 cells were still used as representatives for apoptosis experiments. MCF-7 cells were seeded onto 6-well plates at a density of 1.5×10^5 cells per well. The 6-well plates described above were incubated overnight in a 37 °C, 5% CO_2, and humidified incubator environment. Fresh medium was swapped into the wells, and Mel and Mel@PHA-PhaC were added to their respective wells at a final concentration of 1 μmol/L. At the same time, a control group without peptides was established. After 24 h of incubation, the medium containing the peptide was removed and washed with PBS at 4 °C. Cells were digested using EDTA-free trypsinization and then centrifuged at 2,000 rpm for 5 min. The cells were subsequently stained using an apoptosis kit (Absin, Shanghai, China). Apoptosis was detected using confocal laser scanning microscopy (ZEISS LSM 880, Munich, Germany) and flow cytometry (Beckman, USA).

3. Results and discussion

3.1 Screening of the cationic peptide with high anticancer activity

Cationic peptides from various biological sources or designed rationally demonstrate different levels of cytotoxic activity against cancer cells [25]. First, Mel extracted from the venom of the European honey bee and CM4 extracted from the hemolymph of the silkworm Bombyx mori, along with two other peptides, CMt and RALA, were rationally designed, were investigated for their anticancer properties against various types of cancer cells. The MTT assay results for the four peptides on HepG2, MCF-7, Hela, MGC-803, and Aspc-1 cancer cells are depicted in Fig. 1. Mel exhibited a dose-dependent cytotoxic effect on all five cancer cell lines, while CM4, CMt, and RALA demonstrated less potent inhibitory effects on these cancer cells. The inhibitory effect of CM4, CMt, and RALA peptides at any concentration on the five cancer cells was not significant, as the cell viability remained higher than 71.7%. A comparable inhibitory effect of Mel was also observed at a concentration of 1 μmol/L, resulting in a cell viability of 85.2%. However, when the concentration of Mel was increased to 3 μmol/L, the cell viability of the other four cells was significantly reduced by approximately 50%. When the concentration reached 5 μmol/L, Mel exhibited a highly significant cell inhibitory effect, resulting in cell viability values of 11.1%, 3.3%, 3.3%, 33.2%, and 0.3% for HepG2, MCF-7, Hela, MGC-803, and Aspc-1 cells, respectively. Currently, there are reports on the anti-tumor effects of Mel on HepG2 and MCF-7 cells, with the peptide dosage ranging from 5–10 μg/mL and 0.5-2 μg/mL, respectively [26, 27]. This indicates that our research results are in line with existing reports. The anticancer effect of Mel on cervical cancer (Hela) cells, gastric cancer (MGC-803) cells, and pancreatic cancer (Aspc-1) cells has not been studied. Our research also broadens the understanding of the types of cells affected by Mel. In addition, the anticancer effects of RALA and CMt alone have not been widely researched [28, 8]. These two cationic peptides, along with the previously reported CM4, do not exhibit a significant inhibitory effect on cancer cell growth at low concentrations (< 5 μmol/L). Even if reaching a high concentration of 20 μmol/L can reduce cell viability by 50% [29], it is still much inferior to Mel, which exhibits excellent effects at low doses. As a result, Mel was selected for further research.

3.2 *Construction of Mel@PHA-PhaC microspheres with SUMO tag assembled in E. coli*

Mel has rapid kinetics of action and a short systemic half-life in vivo, which limits its therapeutic potential in the clinic. On the other hand, limited yields from prokaryotic expression can also restrict its application [30]. To preserve the structure of Mel to maintain its biological activity, and increase its yield, a microsphere of Mel was designed and synthesized in engineered *E. coli*. We utilize the capability to functionally modify and extensively synthesize the surface of the PHA microsphere in *E. coli* to display Mel on the microsphere surface [31]. Thus, a plasmid

containing both the gene related to PHA microsphere synthesis and the Mel synthesis gene was designed (Fig. 1A). To enhance the expression and solubility of Mel, a SUMO tag was attached to its N-terminus. The genes related to PHA microsphere synthesis include *phaA*, *phaB*, and *phaC*, which encode the β-ketothiolase (PhaA), (R)-specific acetoacetyl-CoA reductase (PhaB), and PHA synthetase (PhaC), respectively [32]. After connecting *phaC* with the *Mel* gene through the G4S linker, the fused PhaC and Mel proteins were expressed on the surface of microspheres in *E. coli*. According to the design, the phaA and phaB genes were amplified from the pET-28a *phaABC* plasmid previously constructed in our laboratory and inserted into the BamHI and HindIII restriction sites in the multiple cloning site 1 (MCS1) of pACYCdDuet-1. Subsequently, the amplified phaC and mel genes were simultaneously inserted into the XhoI and KpnI restriction sites in MCS2 of pACYCdDuet-1 using the seamless cloning kit. The recombinant plasmid pACYCdDuet-1 *phaAB* & *sumo-mel-phaC* was confirmed through restriction enzyme digestion and agarose gel electrophoresis analysis, which demonstrated the correct insertion of the genes *phaAB* and *sumo-mel-phaC* into the corresponding site of the vector (Fig. 2A). Furthermore, gene sequencing confirmed the accurate construction of the plasmid.

The correct recombinant plasmid mentioned above was transformed into *E. coli*. The expression of the fusion protein SUMO-Mel-PhaC and the production of Mel@PHA-PhaC microspheres with SUMO tags by the induced recombinant *E. coli* were confirmed through SDS-PAGE and Sudan black staining. The SDS-PAGE assay revealed that the strain was capable of expressing the fusion protein SUMO-Mel-PhaC, which had a molecular weight of approximately 80 kDa (Fig. 2B). Sudan black staining confirmed that the strain produced microspheres within the cell (Fig. 2C). Furthermore, the SEM analysis confirmed the presence of microspheres ranging in diameter from 100 to 800 nm (Fig. 2D).

3.3 Purification and characterization of Mel@PHA-PhaC microspheres

The purification process of Mel@PHA-PhaC is depicted in Fig. 3. Mel@PHA-PhaC microspheres with SUMO tags, produced by *E. coli*, were purified using sucrose density gradient centrifugation and then analyzed by SDS-PAGE. A protein band with a size of 80 kDa was observed in lane 2 (Fig. 4A), which closely matched the molecular weight of the SUMO-Mel-PhaC fusion protein (theoretical molecular mass calculated as 81.2 kDa). Therefore, this indicates that the fusion protein SUMO-Mel-PhaC was indeed present on the extracted microspheres, with higher purity and fewer miscellaneous proteins. As the SUMO tag (11.3 kDa) was still attached to the fusion protein of the Mel@PHA-PhaC microsphere, in order to prevent its interference with subsequent experiments, the Ulp1 protein was used to remove it. The Ulp1 protein, successfully purified by Ni^{2+}-NTA chromatography (Fig. 4B), was diluted to 40 μg/mL and then digested with the extracted PHA microspheres at a volume ratio of 1:10 for SUMO-tagged digestion. Finally, the SUMO tag was successfully removed, and a microsphere, Mel@PHA-PhaC, containing only Mel-PhaC, was successfully obtained (Fig. 4C). The fusion protein Mel-PhaC content on microspheres was determined to be 97.4 μg/mg using protein electrophoresis with BSA calibration (Fig. 4D). The Mel content was found to be 4 μg/mg, which is slightly lower than the reported Mel loading of 6.4 nmol/mg (17.92 μg/mg) in calcium carbonate microspheres [33].

In addition, the size and morphology of Mel@PHA-PhaC were examined by SEM and TEM. It can be observed from the SEM analysis that the Mel@PHA-PhaC morphology is spherical, with uniformly sized particles of about 300 nm (Fig. 4E). As depicted in the TEM image, the interior of the microphere is a compact and dense structure, with a thin layer on the surface, which may be fusion proteins attached to the surface (Fig. 4F).

3.4 *In vitro cytotoxicity assessment of Mel@PHA-PhaC*

To confirm the continued anticancer effect of Mel@PHA-PhaC microspheres, we conducted MTT testing. The effect of various concentrations of free Mel peptides (1, 2, 3, 4, 5 μmol/L) and Mel@PHA-PhaC microspheres (0.1, 0.5, 1.0, 1.5, 2.0 μmol/L) on the activity of cancer cell lines (HepG2, MCF-7, Hela, MGC-803, Aspc-1) was examined. A concentration-dependent increase in cytotoxicity was observed in all five cell types following treatment with free Mel or Mel@PHA-PhaC (Fig. 5A, B). Mel@PHA-PhaC exhibited almost similar cell cytotoxicity compared to free Mel (1–5 μmol/L) at a concentration of 0.1-2.0 μmol/L in HepG2, MCF-7, and Hela cells. For MGC-803 cells, the cell viability of Mel@PHA-PhaC at a concentration of 2 μmol/L was significantly lower than that of free Mel at 5 μmol/L, with viabilities of 2.7% and 33.2%, respectively. When it comes to Aspc-1 cells, the cell viability of Mel@PHA-PhaC at a concentration of 0.1 μmol/L was nearly 48.4% lower than that of free Mel at a concentration of 1 μmol/L. As the concentration of Mel@PHA-PhaC continued to increase to 2 μmol/L, cell viability exhibited a much more gradual decline. In contrast, when the concentration of free Mel was higher than 2 μmol/L, cell viability sharply declined, with values dropping to less than 11.0%, and almost all cells died at a concentration of 5 μmol/L. The IC50 values for free Mel and Mel@PHA-PhaC were 1.49 μM and 0.07 μM, respectively (Fig. 5C). These findings confirm that the Mel@PHA-PhaC microsphere exhibits excellent anticancer activity. In addition, the sensitivity of various cancer cells to Mel@PHA-PhaC varies with concentration, necessitating different treatment approaches for drug administration in the future.

To visually assess the effect of free Mel and Mel@PHA-PhaC on cell growth, calcein AM/PI staining was performed with MCF-7 cells. Calcein AM is a non-fluorescent dye that can permeate cells. It is converted to calcein by the esterase activity of live cells, resulting in green fluorescence and indicating an intact plasma membrane. The nucleic acid red fluorescent dye propidium iodide (PI) can only stain dead cells with disrupted membrane integrity because it cannot penetrate the membrane of living cells. Therefore, the combination of calcein AM and PI can be used for dual fluorescence staining to simultaneously detect cell viability and cytotoxicity in both living and dead cells. As shown in Fig. 5D, the presence of green fluorescence in cells treated with PBS alone indicated that the cell membrane was intact and unaffected. After treatment with Mel, nearly all cancer cells returned to a normal state, with only a small number of cells dying and being stained red by PI. The cancer cells were nearly all deceased after treatment with Mel@PHA-PhaC microspheres, which were predominantly red after staining, with only a few cells appearing green.

3.5 *Trypsin stability assay*

Natural peptides are easily hydrolyzed by proteases in vivo, resulting in a short half-life. However, nanostructures stabilize the peptide and reduce the degradation reaction. To assess the functional stability of the microspheres, free Mel and Mel@PHA-PhaC were treated with 1 mg/mL of trypsin. Since Mel and Mel@PHA-PhaC had the same effect on the activity of Aspc-1 cells at a concentration of 2 μmol/L, this condition was used for peptide stability verification. In the absence of trypsin treatment, the cell survival rate was approximately 8.5% when treated with both Mel and Mel@PHA-PhaC (Fig. 6). In contrast, the survival rate of cancer cells was 84.8% after free Mel was digested by trypsin at 37 °C for 4 h, indicating that free peptides nearly lose their original activity after digestion. Cancer cells were treated with Mel@PHA-PhaC digested with trypsin, which resulted in a cell survival rate of 21%. This suggests that the structure of the microspheres effectively protects Mel from trypsin degradation, enabling it to maintain most of its anticancer activity. This may be because Mel-PhaC fusion proteins bind to PHA microspheres through covalent bonds. This indicates that the Mel on the PHA microsphere is effectively protected by fusing with PhaC, thus preventing trypsin recognition. It is also possible that the three-dimensional structure of the fusion protein conceals Mel within the PhaC protein, thereby avoiding protease degradation. As previously reported, no protein digestion products were observed in the mass spectra after digestion of Melittin–lipid disk mixtures with

trypsin at 25 ℃ for 40 min [34]. Our Mel@PHA-PhaC microsphere has a longer digestion time than previously reported, lasting up to 4 h without being affected, further indicating excellent structural stability.

3.6 *Apoptosis*

Mel@PHA-PhaC or Mel induced apoptosis of cancer cells was assessed using flow cytometry. Annexin V is a phospholipid-binding protein that has a high affinity for phosphatidylserine. Therefore, it can bind to the cell membrane of cells in the early stage of apoptosis through the exposed phosphatidylserine on the outer surface of the cell. PI is a nucleic acid dye that is unable to penetrate intact cell membranes. However, it can penetrate dead cells and cells in the middle and late stages of apoptosis due to increased membrane permeability, resulting in red-stained nuclei. Therefore, two dyes were used to differentiate cells at different stages of apoptosis. Flow cytometry profiles of MCF-7 cells treated with Mel@PHA-PhaC and Mel (1 μmol/L) are shown in Fig. 7A. The results indicated that the percentages of early and late apoptotic cells in MCF-7 cells following Mel@PHA-PhaC microsphere treatment were 30.8% and 9.2%, respectively, which were higher than the percentages of early and late apoptotic cells after Mel peptide treatment (2.6%, 5.96%). After 24 h of incubation of MCF-7 cells with 1 μmol/L microspheres, more cells exhibited early apoptosis than late apoptosis. There was no significant green and red fluorescence in the control and Mel-treated plates, indicating that the integrity of the cell membrane was not compromised (Fig. 7B). Collectively, these results indicate that Mel@PHA-PhaC exerts antitumor activity on MCF-7 cells, primarily by promoting cell apoptosis. The possible route and mechanism of Mel@PHA-PhaC on a cancer cell is deduced. Mel@PHA-PhaC microsphere can be taken by cells via caveolin-mediated endocytosis or clathrin-caveolin-independent endocytosis, which induce oxidative stress in the cell. When oxidative stress persists or exceeds a certain level, it causes oxidative damage to DNA and lipids, thereby potentially initiating cell death by apoptosis and inhibiting malignant progression [35]. In addition, some studies have suggested that Mel specifically target cancer cells to induce cell death. Mel has been shown to be selective for triple-negative breast cancer and to induce cell death with a low effect on normal cells [36]. Thus, to exploit the targeting of Mel@PHA-PhaC microsphere to triple-negative breast cancer would be conducted by us in the future.

4. Conclusions

The most significant anti-cancer activity of Mel was identified in natural and rationally designed cationic peptides. The PHA microspheres synthesized by *E. coli* were designed to deliver Mel, facilitating the in situ assembly of Mel on the surface of the PHA microspheres. This approach makes the preparation of Mel nanostructures more convenient. Furthermore, Mel@PHA-PhaC exhibited excellent stability against trypsin and demonstrated promising anticancer effects on five different types of cancer cells in vitro. This study offers valuable insights into the design and application of a PHA microsphere-based peptide delivery system for producing stable and enhanced peptides for cancer therapy. In the future, we will continue to enhance the expression of ACPs on microspheres to increase the peptide loading capacity and truly achieve large-scale production of nanostructured peptides within cells.

Declarations

Acknowledgments. This research was funded by the Natural Science Foundation of China (grant number 3210120332), the Natural Science Foundation of Hebei Province (B2023201108), the Research and Innovation Team Project of Hebei University (IT2023B01) and the Post-graduate's Innovation Fund Project of Hebei University (grant number HBU2023SS013).

Author Contributions. Conceptualization: X.F., W.L., H.Z. and S.F.; methodology: X.F., C.Z., S.F., S.W., J.D. and S.M.; validation: X.F., C.Z., S.F., S.W., and S.M.; formal analysis: X.F., C.Z.; resources: J.D., W.L. and H.Z.; data curation: X.F. and S.F.; writing—original draft preparation: X.F.; writing—review and editing: X.F., J.D., W.L. and H.Z.; supervision: J.D., W.L. and H.Z.; funding acquisition: W.L. and H.Z. All authors have read and agreed to the published version of the manuscript.

Disclosure of Interest: The authors have no competing interests to declare that are relevant to the content of this article.

References

1. Tornesello, A.L., Borrelli, A., Buonaguro, L., Buonaguro, F.M., Tornesello, M.L.: Antimicrobial peptides as anticancer agents: functional properties and biological activities. Molecules. **25**(12), 2850 (2020)
2. Hancock, R.E.W., Sah, H-G.: Antimicrobial and host-defense peptides as new anti-infective therapeutic strategies. Nat. Biotechnol. **24**, 1551-1557 (2006)
3. Dorschner, R.A., Pestonjamasp, V.K., Tamakuwala, S., Ohtake, T., Rudisill, J., Nizet, V., Agerberth, B., Gudmundsson, G.H., Gallo, R.L.: Cutaneous injury induces the release of cathelicidin anti-microbial peptides active against group a streptococcus. J. Invest. Dermatol. **117**(1), 91-97 (2001)
4. Raghuraman, H., Chattopadhyay, A.: Melittin: a membrane-active peptide with diverse functions. Bioscience. Rep. **27**(4-5), 189–223 (2007)
5. Li, C., Liu, H., Yang, Y., Xu, X., Lv, T., Zhang, H., Liu, K., Zhang, S., Chen, Y.: N-myristoylation of antimicrobial peptide CM4 enhances its anticancer activity by interacting with cell membrane and targeting mitochondria in breast cancer cells. Front. Pharmacol. **9**, 1297 (2018)
6. Isogai, E., Isogai, H., Takahashi, K., Okumura, K., Savage, P.B.: Ceragenin CSA-13 exhibits antimicrobial activity against cariogenic and periodontopathic bacteria. Oral. Microbiol. Immunol. **24**, 170-172 (2009)
7. McCarthy, H.O., McCaffrey, J., McCrudden, C.M., Zholobenko, A., Ali, A.A., McBride, J.W., Massey, A.S., Pentlavalli, S., Chen, K.-H., Cole, G., Loughran, S.P., Dunne, N.J., Donnelly, R., Kett, V.L., Robson, T.: Development and characterization of self-assembling nanoparticles using a bio-inspired amphipathic peptide for gene delivery. J. Control. Release. **189**, 141-149 (2014)
8. Chen, Y.Q., Zhang, S.Q., Li, B.C., Qiu, W., Jiao, B., Zhang, J., Diao, Z.Y.: Expression of a cytotoxic cationic antibacterial peptide in *Escherichia coli* using two fusion partners. Protein. Expres. Purif. **57**(2), 303-311 (2008)
9. Gaspar, D., Veiga, A.S., Castanho, M.A.R.B.: From antimicrobial to anticancer peptides. Front. Microbiol. **4**, 294 (2013)
10. Rodríguez, A.A., Otero-González, a., Ghattas, M., Ständker, L.: Discovery, optimization, and clinical application of natural antimicrobial peptides. Biomedicines. **9**(10), 1381 (2021)
11. Biswaro, L.S., da Costa Sousa, M.G., Rezende, T.M.B., Dias, S.C., Franco, O.L.: Antimicrobial peptides and nanotechnology, Recent Advances and Challenges. Front. Microbiol. **9**, 855 (2018)
12. Leite, M.L., da Cunha, N.B., Costa, F.F.: Antimicrobial peptides, nanotechnology, and natural metabolites as novel approaches for cancer treatment. Pharmacol. Therapeut. **183**, 160-176 (2018)
13. Pandaab, J.J., Chauhan, V.S.: Short peptide based self-assembled nanostructures: implications in drug delivery and tissue engineering. Polym. Chem. **5**, 4418-4436 (2014)

14. Niemirowicz, K., Prokop, I., Wilczewska, A.Z., Wnorowska, U., Piktel, E., Wątek, M., Savage, P.B., Bucki, R.: Magnetic nanoparticles enhance the anticancer activity of cathelicidin LL-37 peptide against colon cancer cells. Int. J. Nanomed. **10**, 3843-3853 (2015)
15. Soman, N.R., Lanza, G.M., Heuser, J.M., Schlesinger, P.H., Wickline, S.A.: Synthesis and characterization of stable fluorocarbon nanostructures as drug delivery vehicles for cytolytic peptides. Nano Lett. **8**(4), 1131-1136 (2008)
16. Jiang, J.W., Pan, Y.Z., Li, Z.Y., Xia, L.J.: Cecropin-loaded zeolitic imidazolate framework nanoparticles with high biocompatibility and cervical cancer cell toxicity. Molecules. **27**(14), 4364 (2022)
17. Li, Z., Loh, X.J.: Recent advances of using polyhydroxyalkanoate-based nanovehicles as therapeutic delivery carriers. Wires. Nanomed. Nanobi. **9**, 1249 (2016)
18. Draper, J.L., Rehm, B.H.: Engineering bacteria to manufacture functionalized polyester beads. Bioengineered. **3**(4), 203-208 (2012)
19. Chen, G.Q.: A microbial polyhydroxyalkanoates (PHA) based bio- and materials industry. Chem. Soc. Rev. **38**(8), 2434-2446 (2009)
20. Madkour, M.H., Heinrich, D., Alghamdi, M.A., Shabbaj, I.I., Steinbüchel, A.: PHA Recovery from Biomass. Biomacromolecules. **14**(9), 2963-2972 (2013)
21. Thankappan, B., Sivakumar, J., Asokan, S., Ramasamy, M., Pillai, M.M., Selvakumar, R., Angayarkanni, J.: Dual antimicrobial and anticancer activity of a novel synthetic α-helical antimicrobial peptide. Eur. J. Pharm. Sci. **161**, 105784 (2021)
22. Tian, J.M., Sinskey, A.J., Stubbe, J.A.: Kinetic studies of polyhydroxybutyrate granule formation in wautersia eutropha H16 by transmission electron microscopy. J. Bacteriol. **187**(11), 3814-3824 (2005)
23. Cai, S.F., Cai, L., Liu, H.L., Liu, X.Q., Han, J., Zhou, J., Xiang, H.: Identification of the haloarchaeal phasin (PhaP) that functions in polyhydroxyalkanoate accumulation and granule formation in haloferax mediterranei. Appl. Environ. Microb. **78**(6), 1946-1952 (2012)
24. Li, S.J., Yang, Y.K., Liu, M., Bai, Z.H., Jin, J.: Efficient expression of SUMO protease Ulp1 and used to express and purified scFv by His-SUMO tag. China. Biotech. **38**(3), 51-61 (2018)
25. Riedl, S., Zweytick, D., Lohner, K.: Membrane-active host defense peptides-Challenges and perspectives for the development of novel anticancer drugs. Chem. Phys. Lipids. **164**(8), 766-781 (2011)
26. Zhang, H., Zhao, B., Huang, C., Meng, X.M., Bian, E.B., Jun, L.: Melittin restores PTEN expression by down-regulating HDAC2 in human hepatocelluar carcinoma HepG2 cells. PLos. One. **9**(5), e95520 (2014)
27. Wang, J.J., Li, F.Y., Tan, J., Peng, X.W., Sun, L.L., Wang, P., Jia, S.N., Yu, Q.M., Huo, H.L., Zhao, H.Y.: Melittin inhibits the invasion of MCF-7 cells by downregulating CD147 and MMP-9 expression. Oncol. Lett. **13**, 599-604 (2017)
28. Bennett, R.; Yakkundi, A.; McKeen, H.D.; McClements, L.; McKeogh, T.J.; McCrudden, C.M.; Arthur, K.; Robson, T.; McCarthy, H.O. RALA-mediated delivery of FKBPL nucleic acid therapeutics. Nanomedicine. **10**(19), 2989-3001 (2015)
29. Chen, Y.Q., Min, C., Sang, M., Han, Y.Y., Ma, X., Xue, X.Q., Zhang, S.Q.: A cationic amphiphilic peptide ABP-CM4 exhibits selective cytotoxicity against leukemia cells. Peptides. **31**(8), 1504-1510 (2010)
30. Liu, C.C., Hao, D.J., Zhang, Q., An, J., Zhao, J.J., Chen, B., Zhang, L.L., Yang, H.: Application of bee venom and its main constituent melittin for cancer treatment. Cancer. Chemoth. Pharm. **78**, 1113-1130 (2016)

31. Sharma, V., Sehgal, R., Gupta, R.: Polyhydroxyalkanoate (PHA): properties and modifications. Polymers. **212**, 123161 (2012)
32. de Melo, R.N., de Souza Hassemer, G., Steffens, J., Junges, A., Valduga, E.: Recent updates to microbial production and recovery of polyhydroxyalkanoates. 3 Biotech. **13**(6), 204 (2023)
33. Yazdian Robati, R., Arab, A., Ramezani, M., Rafatpanah, H., Bahreyni, A., Nabavinia, M.S., Abnous, K., Taghdisi, S.M.: Smart aptamer-modified calcium carbonate nanoparticles for controlled release and targeted delivery of epirubicin and melittin into cancer cells in vitro and in vivo. Drug Dev. Ind. Pharm. **45**(4), 603-610 (2019)
34. Zetterberg, M.M., Reijmar, K., Pränting, M., Pränting, Å., Andersson, D.I., Edwards, K.: PEG-stabilized lipid disks as carriers for amphiphilic antimicrobial peptides. J. Control. Release **156**(3), 323-328 (2011)
35. Yu, X., Jia, S., Yu, S., Chen, Y., Zhang. C., Chen, H., Dai, Y.: Recent advances in melittin-based nanoparticles for antitumor treatment: from mechanisms to targeted delivery strategies. J. Nanobiotechnol. **21**,454 (2023)
36. Daniluk, K., Lange, A., Wójcik, B., Zawadzka, K., Bałaban, J., Kutwin, M., Jaworski, S.: Effect of Melittin complexes with graphene and graphene oxide on triple-negative breast cancer tumors grown on chicken embryo chorioallantoic membrane. Int. J. Mol. Sci. **24**, 8388 (2023)

Figures

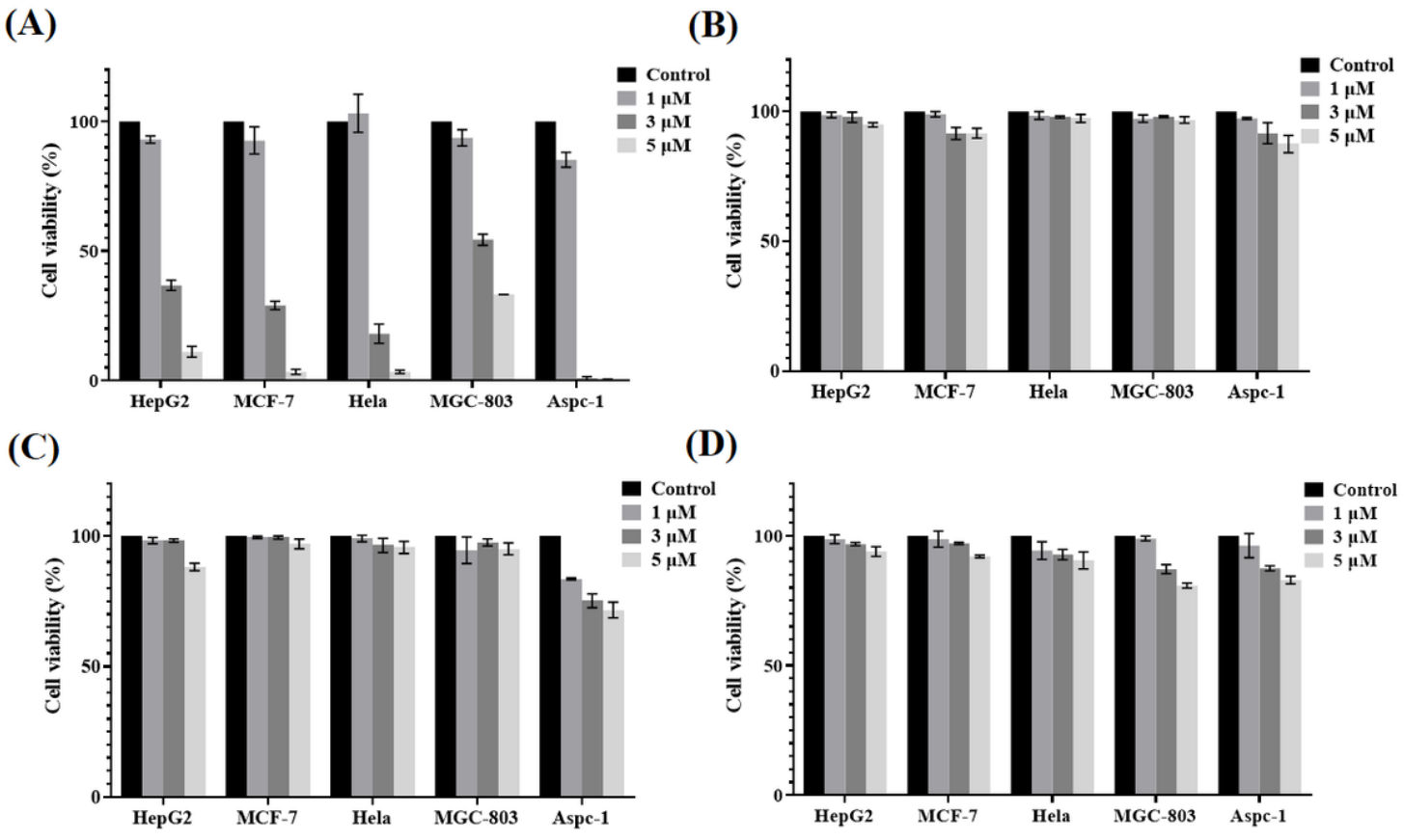

Figure 1

Cytotoxicity (MTT) assay for four free peptides: (A) Mel, (B) CM4, (C) RALA, and (D) CMt against HepG2, MCF-7, Hela, MGC-803, and Aspc-1 cell lines.

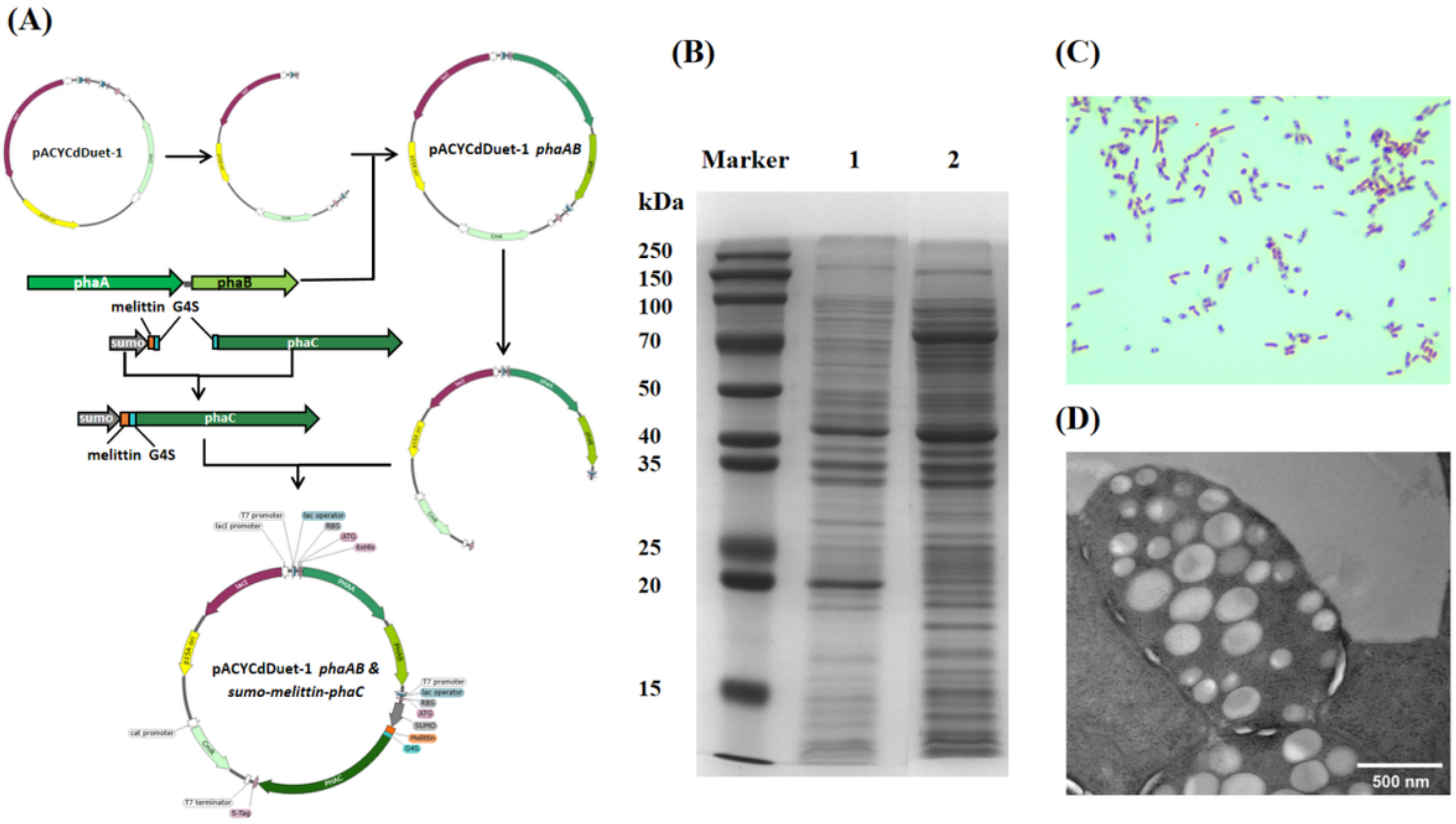

Figure 2

Synthesis of PHA microspheres in *E. coli*. (A) Construction of the pACYCdDuet-1 phaAB & sumo-mel-phaC plasmid. (B) SDS-PAGE analysis was conducted to assess the expression of the fusion protein SUMO-PhaC-Mel by the induced recombinant *E. coli*. Lane Marker, protein molecular weight standard. Lane 1, recombinant *E. coli* before induction. Lane 2, total protein levels after induction with 1 mmol/L IPTG. (C) Sudan black staining and (D) SEM image of Mel@PHA-PhaC microspheres with SUMO tags within *E. coli* after induction.

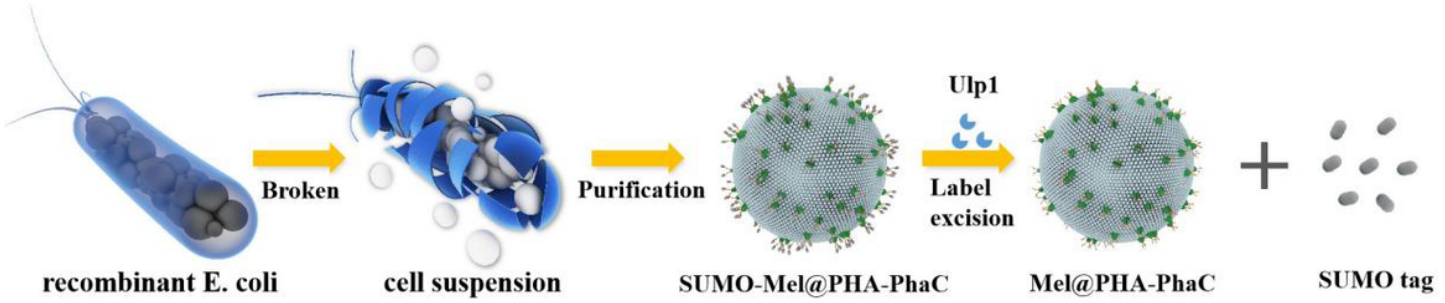

Figure 3

The purification process of the Mel@PHA-PhaC microspheres.

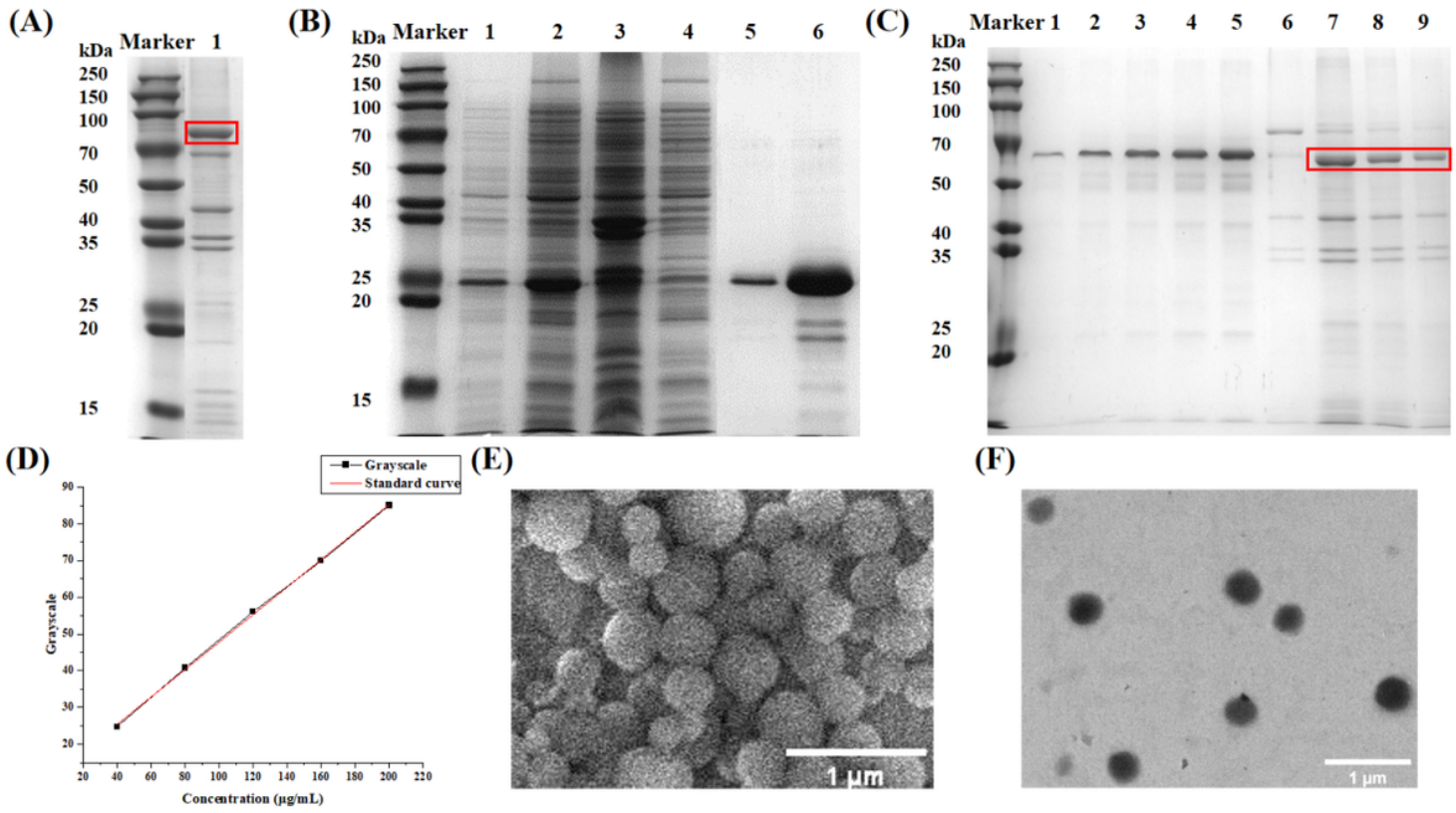

Figure 4

(A) SDS-PAGE analysis of purified Mel@PHA-PhaC microspheres. Lane 1, total protein levels after induction with 1 mmol/L IPTG. (B) SDS-PAGE analysis of purified Ulp1 protein. Lane 1, total protein levels after induction with 0.5 mmol/L IPTG. Lane 2, the supernatant of the cell lysate. Lane 3, precipitation of the cell lysate. Lane 4, protein fractions flowed through from the Ni^{2+}-NTA. Lane 5, Ulp1 protein. Lane 6, concentrated Ulp1 protein. (C) SDS-PAGE analysis of Mel-PhaC fusion proteins after Ulp1 digestion. Lane 1, 40 μg/mL of BSA. Lane 2, 80 μg/mL of BSA. Lane 3, 120 μg/mL of BSA. Lane 4, 160 μg/mL of BSA. Lane 5, 200 μg/mL of BSA. Lane 6, SUMO-Mel-PhaC fusion proteins after a fivefold dilution. Lane 7, Mel-PhaC fusion proteins. Lane 8, Mel-PhaC fusion proteins after a twofold dilution. Lane 9, Mel-PhaC fusion proteins after a fourfold dilution. (D) Grayscale standard curve for BSA. (E) TEM image of the Mel@PHA-PhaC microsphere. (F) SEM image of the Mel@PHA-PhaC microsphere.

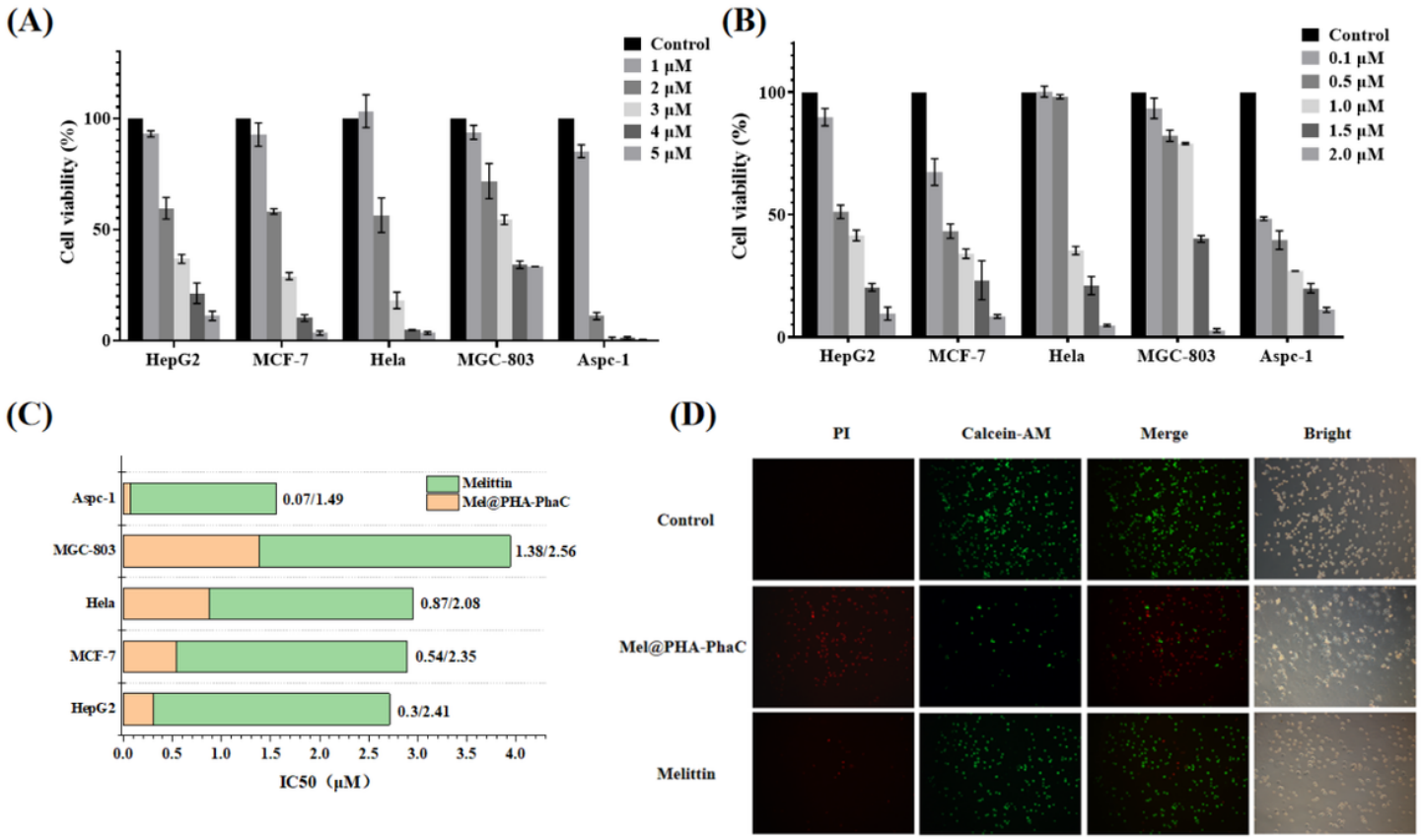

Figure 5

Cytotoxicity assay of (A) Mel and (B) Mel@PHA-PhaC microspheres against HepG2, MCF-7, Hela, MGC-803, and Aspc-1 cell lines. (C) IC50 values of five cancer cells for Mel and Mel@PHA-PhaC. (D) Fluorescent microscopic images of Mel and Mel@PHA-PhaC treated with MCF-7 cells. Green represents live cells stained with calcein AM, while red represents the dead cells stained with PI.

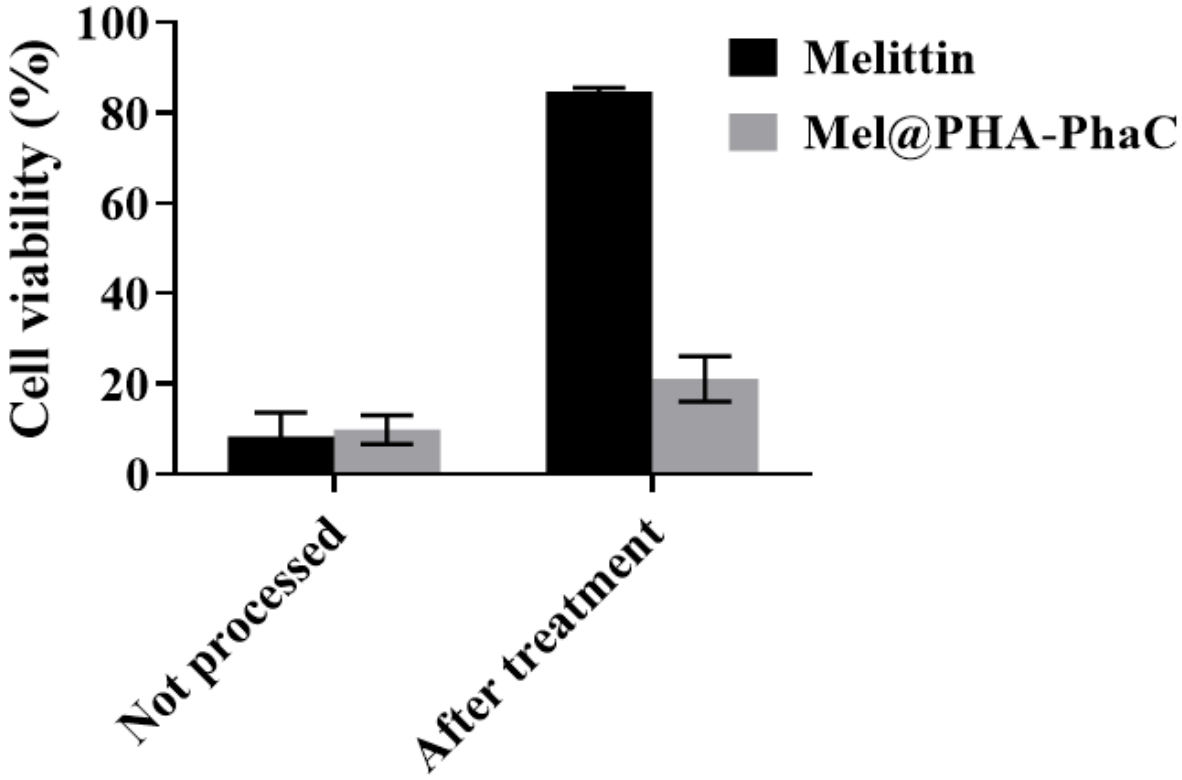

Figure 6

Effect of Mel@PHA-PhaC and Mel at concentrations of 2 μmol/L before and after treatment with pancreatic enzymes on Aspc-1 cell activity.

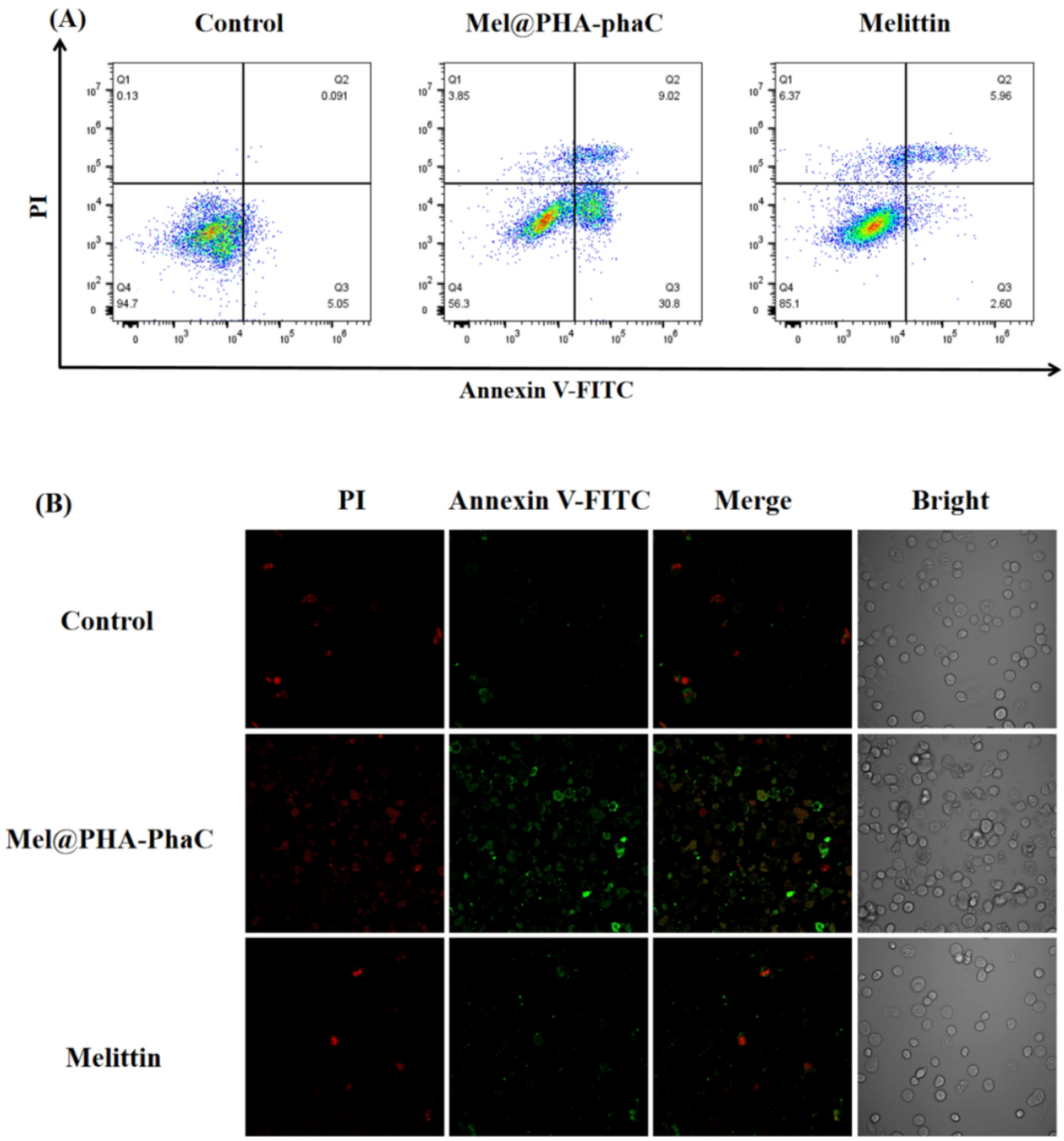

Figure 7

(A) The effect of Mel@PHA-PhaC and Mel induced apoptosis in MCF-7 cells using Annexin V/PI staining by flow cytometry. (B) Representative fluorescence microscopic images show Annexin V-FITC (green) and PI (red) staining after incubating MCF-7 cells with Mel@PHA-PhaC and Mel.